Structural Monitoring and Maintenance, *Vol. 1, No. 1 (2014) 089-110*
DOI: http://dx.doi.org/10.12989/smm.2014.1.1.089

Iterative damage index method for structural health monitoring

Taesun You[1], Paolo Gardoni[2] and Stefan Hurlebaus[*3]

[1]*Texas A&M Transportation Institute, College Station, TX 77843-3135, USA*
[2]*Department of Civil and Environmental Engineering, University of Illinois at Urbana-Champaign, Urbana, IL61801-2351, USA*
[3]*Zachry Department of Civil Engineering, Texas A&M University, College Station, TX 77843-3136, USA*

(Received March 3, 2014, Revised March 15, 2014, Accepted March 24, 2013)

Abstract. Structural Health Monitoring (SHM) is an effective alternative to conventional inspections which are time-consuming and subjective. SHM can detect damage early and reduce maintenance cost and thereby help reduce the likelihood of catastrophic structural events to infrastructure such as bridges. After reviewing the Damage Index Method (DIM), an Iterative Damage Index Method (IDIM) is proposed to improve the accuracy of damage detection. These two damage detection techniques are compared based on damage on two structures, a simply supported beam and a pedestrian bridge. Compared to the traditional damage detection algorithm, the proposed IDIM is shown to be less arbitrary and more accurate.

Keywords: vibration-based damage identification method; damage index method; damage detection algorithm; structural health monitoring

1. Introduction

Recently, effective inspection and maintenance for infrastructure are placing great importance because infrastructures are deteriorating after construction due to fatigue and corrosion. The Bureau of Transportation Statistics (2008) reported that nearly 26 percent of the bridges in the U.S. are substandard. Traditional inspection procedures for bridges generally rely on subjective and irregular visual examination. As such, there are variations in the inspection results even for the same structure because of the differences in inspectors' experience and judgment. Visual checking is also apt to be a schedule-based inspection process. Discrete inspection processes can fail to detect hidden effects of poor design or maintenance that can be the source of sudden and dangerous events such as a bridge collapse. Between 1989 and 2000, out of 65 bridge failures (caused by design, detailing, construction, maintenance, or material problems), 43 failures were attributed to poor maintenance (Wardhana and Hadipriono 2003). As an alternative to periodic inspections, structural health monitoring (SHM) is a continuous process (Hurlebaus and Gaul 2006) that can detect damage early, reduce the cost of repair and rehabilitation, and help reduce the chance of catastrophic events with the structures.

A number of studies have sought to improve the accuracy of damage detection using SHM. Several researchers (Lenzen 2005, Kim and Kawatani 2007, Kim *et al*. 2008, Mizuno *et al.* 2008,

*Corresponding author, Associate Professor, E-mail: shurlebaus@civil.tamu.edu

http://www.techno-press.org/?journal=smm&subpage=7 ISSN: 2288-6605 (Print), 2288-6613 (Online)

Park *et al*. 2009, Kim *et al*. 2013) have developed damage identification methods using the analysis of dynamic responses of a structure. However, the damage can be estimated where the dynamic responses are recorded. On the other hand, many studies took advantages of the development of instrumentation using sensors that facilitates observation of the dynamic characteristics of a structure, such as frequencies and modeshapes. For example, Pandey *et al*. (1991) proposed to track the changes in modeshapes curvature while Pandey and Biswas (1994) used flexibility changes. Zhang and Aktan (1995) combined the two methods proposed by Pandey *et al*. (1991) and Pandey and Biswas (1994), and developed a method using the changes in flexibility curvature. Shi *et al*. (2000) introduced the correlation between the measured modeshapes change for the undamaged and damaged and the analytical modeshapes change for the undamaged and damaged. If the correlation between the measured modeshapes and analytical changes is unity, the damage is estimated correctly. Despite those efforts, the methods are not practical in infrastructure such as bridges and buildings. This is often the case because small changes in physical properties do not alter frequencies and modeshapes enough to allow their detection. In other case, it is difficult to obtain as many modes as these methods need from these complicated structures. To overcome the limitations, Stubbs and Kim (1996) suggested a Damage Index Method (DIM) using modal strain energy to detect damage.

This paper refers to the measured points on a structure as recording points. Interpolation between selected recording points is then used to make the modeshapes a smooth line. In this paper, the points used in interpolating the modeshapes are called spline points. Note the number of spline points, N_s, is always equal to or greater than the number of recording points, N_r and a cubic spline interpolation function is chosen in this study to avoid Runge's phenomenon which can be occurred when using polynomial interpolation method.

Several researchers (Stubbs and Kim 1996, Stubbs and Park 1996, Kim and Stubbs 2002, Kim *et al.* 2003) verified the accuracy of the DIM with numerical simulation models, while others confirmed its usefulness with experimental evaluation (Park *et al.* 2001, Kim and Stubbs 2003, Kim *et al.* 2007, Choi *et al.* 2008). Moreover, Huang *et al*. (2009) applied the DIM to find the probabilistic capacity and fragility of reinforced concrete columns. Compared with commonly used vibration-based damage detection methods, the DIM is the most accurate (Alvandi and Cremona 2006, Humar *et al.* 2006).

The DIM relies on the calculation of the modal strain energy by measuring the modeshapes of a structure to detect damage. However, the current DIM has two limitations with regard to this calculation. First, the selection of a fixed threshold to determine whether there is enough change in the measurable physical properties to indicate damage in a structure is arbitrary. Second, the damage detection with any fixed threshold is affected by the number of spline points selected.

The purpose of the work described in this paper is to develop a less arbitrary and more accurate vibration-based damage detection method for SHM. A modified DIM, referred to as the Iterative Damage Index Method (IDIM), is proposed. The proposed IDIM does not require defining an arbitrary threshold to identify damage and it is independent of N_s. Thus, the proposed method .promises a generally better and reliable detection of damage.

The remaining of this paper consists of four sections. The technical background is described in the following section. After a brief review of the algorithms used by the current DIM, the proposed IDIM is described. Then, the accuracy of damage prediction using the DIM and the IDIM for a simply supported beam and a pedestrian bridge are compared using numerical and experimental data. Finally, the last section summarizes the findings of this paper and suggests some future work.

2. Damage detection algorithm

First, the quantification of the accuracy of predicted damage by damage identification methods is presented. After that, two damage detection algorithms are explained: DIM and IDIM.

2.1 Damage index method

This section reviews the DIM proposed by Stubbs and Kim (1996). Assuming a structural element can be considered as a Euler-Bernoulli beam (see Fig. 1), the modal strain energy associated to the *i*th mode of undamaged beam, K_i, can be calculated as

$$K_i = \int_0^L EI(x)\left[\phi_i''(x)\right]^2 dx \tag{1}$$

where L is the length of the beam, EI is the flexural rigidity, and ϕ_i'' is the curvature of the *i*th modeshape. Dividing the beam into n segments, the modal strain energy contribution from the *j*th segment to the *i*th mode, k_{ij}, is given by

$$k_{ij} = \int_a^b EI_j\left[\phi_i''(x)\right]^2 dx \tag{2}$$

where the *j*th segment is between $x = a$ and b. As such, the fraction of the *j*th segment's contribution to the total modal strain energy, F_{ij}, can be expressed as

$$F_{ij} = \frac{k_{ij}}{K_i} \tag{3}$$

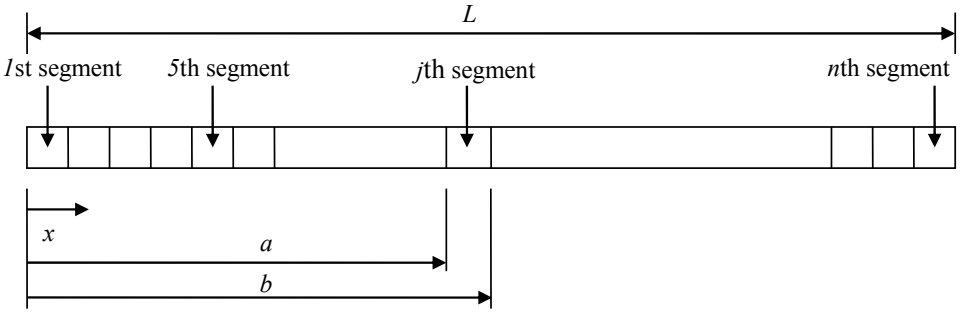

Fig. 1 Structural element with n segmetns

Similarly, for the corresponding damaged element, we have

$$K_i^d = \int_0^L EI^d(x)\left[\phi_i^{d\prime\prime}(x)\right]^2 dx \tag{4}$$

$$k_{ij}{}^d = \int_a^b EI^d{}_j(x)\left[\phi_i^{d\prime\prime}(x)\right]^2 dx \tag{5}$$

$$F_{ij}{}^d = \frac{k_{ij}{}^d}{K_i^d} \tag{6}$$

where the superscript 'd' denotes 'damaged'. Assuming that the fraction of the *j*th element's contribution to the *i*th modal strain energy in the undamaged and damaged structure remains constant (i.e., $F_{ij} = F_{ij}{}^d$), the ratio of the *j*th segment flexural rigidity in the undamaged and damaged structure is given by

$$\zeta_j = \frac{EI_j}{EI_j^d} = \frac{\int_0^L EI(x)\left[\phi_i''(x)\right]^2 dx}{\int_a^b \left[\phi_i''(x)\right]^2 dx} \frac{\int_a^b \left[\phi_i^{d\prime\prime}(x)\right]^2 dx}{\int_0^L EI^d(x)\left[\phi_i^{d\prime\prime}(x)\right]^2 dx} \tag{7}$$

where ζ_j is the damage index for the *j*th segment. For multiple modes, ζ_j is expressed as

$$\zeta_j = \sum_{i=1}^{n_m} \left\{ \frac{\int_0^L EI(x)\left[\phi_i''(x)\right]^2 dx}{\int_a^b \left[\phi_i''(x)\right]^2 dx} \frac{\int_a^b \left[\phi_i^{d\prime\prime}(x)\right]^2 dx}{\int_0^L EI^d(x)\left[\phi_i^{d\prime\prime}(x)\right]^2 dx} \right\} \tag{8}$$

where n_m is the number of modes. Accordingly, the normalized damage index (damage indicator), Z_j, is obtained as

$$Z_j = \frac{\zeta_j - \bar{\zeta}}{\sigma_\zeta} \tag{9}$$

where $\bar{\zeta}$ and σ_ζ are the mean and the standard deviation of the damage index, respectively. For a chosen threshold, $Z_{\text{threshold}}$, if $Z_j \geq Z_{\text{threshold}}$, it is indicated that the *j*th segment is damaged. In this paper, $Z_{\text{threshold}}$ is chosen to be one, meaning that the confidence level for damage detection is 84.1% (Park *et al.* 2001). A flowchart shown in Fig. 2 depicts the entire procedure of the current DIM.

As mentioned in the previous section, there are two crucial restrictions in the use of the DIM. First, the choice of a fixed threshold is arbitrary. Because the particular fixed threshold chosen drives the damage detection results, the selection of the threshold is critical in the DIM. If the selected threshold is smaller than the limit at which actual damage occurs, damage size would be overestimated. In contrast, damage size would be underestimated if the selected threshold is set too

high. As an illustration, in Fig. 3(a) is an appropriate threshold, (b) is a smaller threshold, and (c) is a larger threshold. Although the DIM has this problem with the selection of a fixed threshold to detect damage, various thresholds have been selected. For instance, the threshold was chosen to be one by some researchers (Park *et al.* 2001, Kim and Stubbs 2003, Kim *et al.* 2007, Choi *et al.* 2008, Huang *et al.* 2009) while other researchers selected thresholds of two (Stubbs and Kim 1996, Stubbs and 2002) and three (Kim and Stubbs 2003, Kim *et al.* 2007).

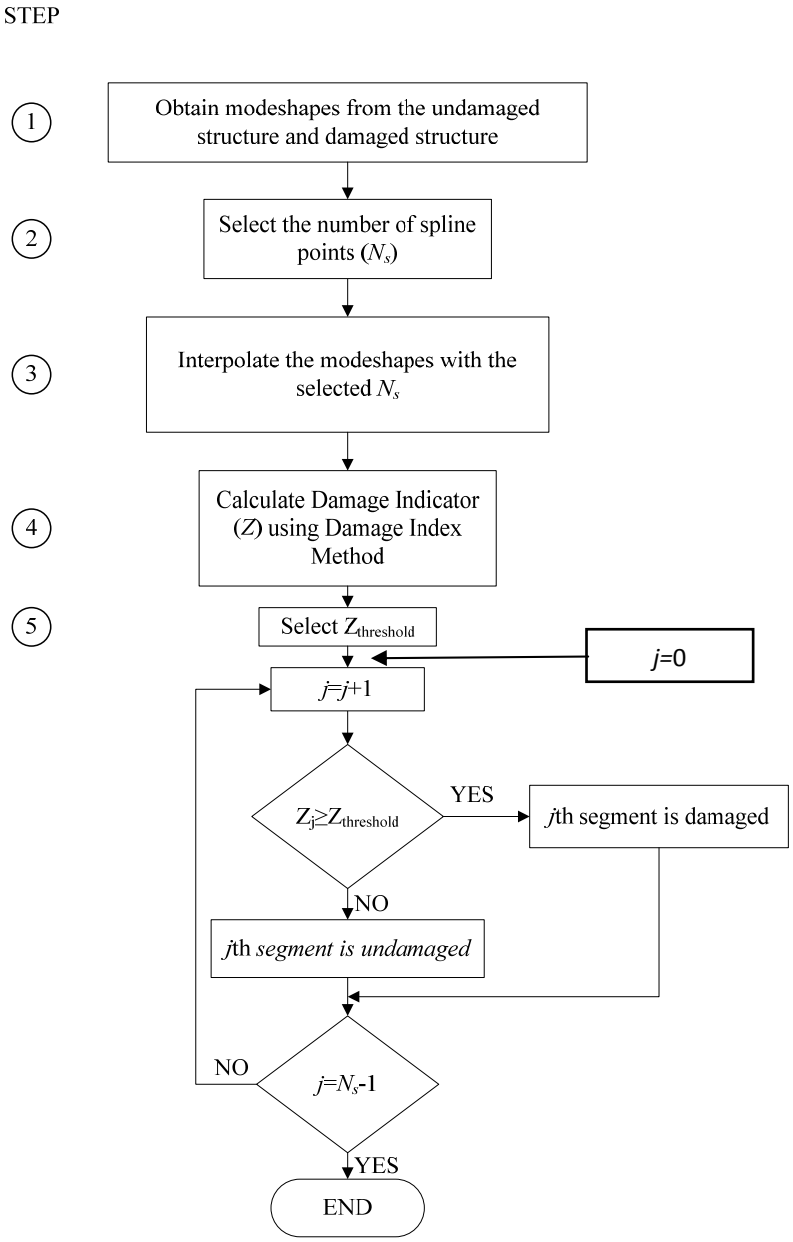

Fig. 2 Flow chart of the Damage Index Method

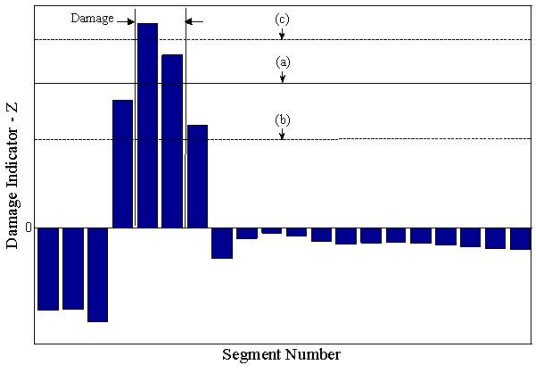

Fig. 3 Damage detection with (a) appropriate threshold, (b) smaller threshold and (c) larger threshold

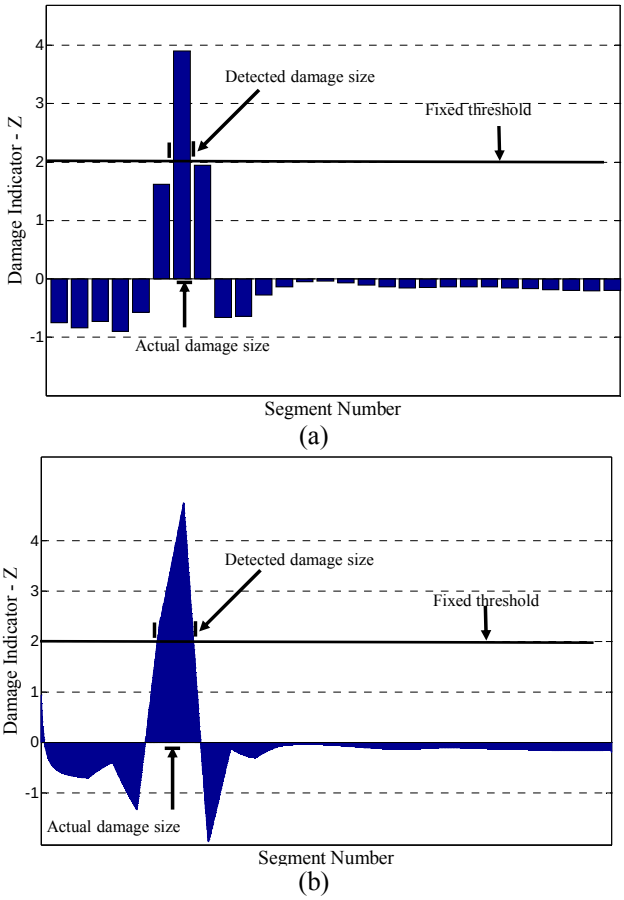

Fig. 4 Damage detection results with (a) N_r recording points and N_{s-1} spline points and (b) N_r recording points and N_{s-2} spline points ($N_{s-1}<N_{s-2}$)

Second, the selection of N_s can influence the results of the damage detection. For example, Fig.

4 illustrates the problem by showing two predicted damage cases with the same N_r but different N_s. Although the damage in the two cases is identical, the damage detection results by the same fixed threshold are different. The extent of damage is detected correctly in Fig. 4(a) while the damage is overestimated in Fig. 4(b).

2.2 Proposed iterative damage index method

The IDIM proposed in this paper overcomes these limitations by relying on the idea that the Z_{ratio} for the same N_r remains constant when different N_s are used. The Z_{ratio} is given by

$$Z_{\text{ratio}} = \frac{\sum_{i=1}^{n_a} Z_{A_i}}{\sum_{j=1}^{n_p} Z_{p_j}} \tag{10}$$

where n_a is the number of damage indicators in an actual damage location, Z_{A_i} is the *i*th damage indicator in an actual damage location, n_p is the number of the positive damage indicators, and Z_{p_j} is the *j*th positive damage indicator. By plotting of N_r and the Z_{ratio}, a fitting function, u_c, is formulated as

$$u_c = 1 - \exp\left(\frac{-N_r}{\tau}\right) \tag{11}$$

where τ is a parameter that needs to be estimated. Unfortunately, τ varies with different damage sizes. To solve the problem, we introduce a new parameter, C, that remains constant over different damage sizes and is defined as

$$C = \ell \times \tau \tag{12}$$

where ℓ is the damage size. In this paper, it is assumed that C is unchanged corresponding to the change in damage size.

Fig. 5 gives a flowchart for the IDIM. The first four steps of the proposed method are the same as those of the current DIM (see Figs. 2 and 5). The sum of the positive damage indicators, Z_{sum}, is given by

$$Z_{\text{sum}} = \sum_{j=1}^{np} Z_{p_j} \tag{13}$$

After numbering the positive damage indicators in descending order (i.e. Z_{p1} = maximum of the Z_{pj}), the sum of the first k positive damage indicator(s), Z'_{sum}, can be calculated as

$$Z'_{\text{sum}} = \sum_{j=1}^{k} Z_{pj} \tag{0}$$

where k is the iteration number. Thus, the ratio of the sum of the positive damage indicators to the sum of the first k positive damage indicator(s), Z_{ratio}, is expressed as

$$Z_{\text{ratio}} = \frac{Z'_{\text{sum}}}{Z_{\text{sum}}} \tag{15}$$

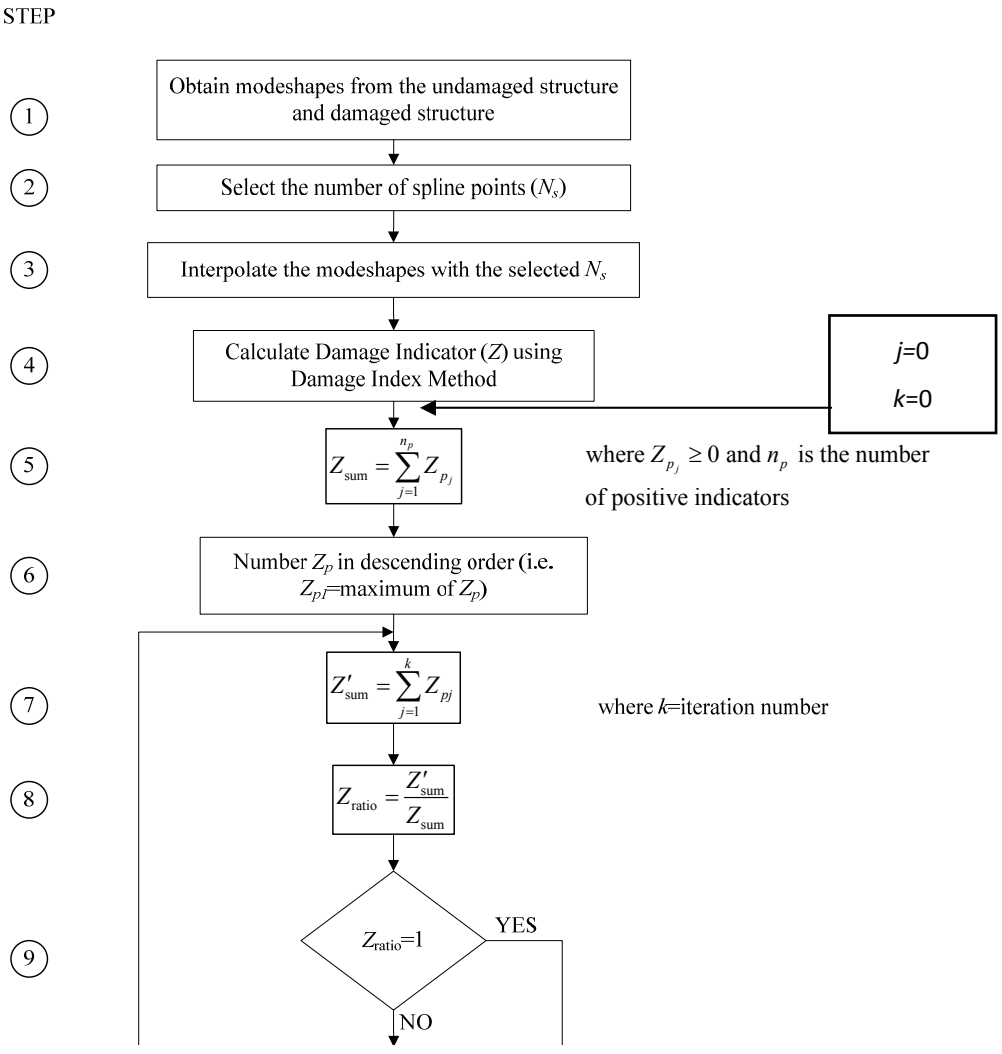

Continued-

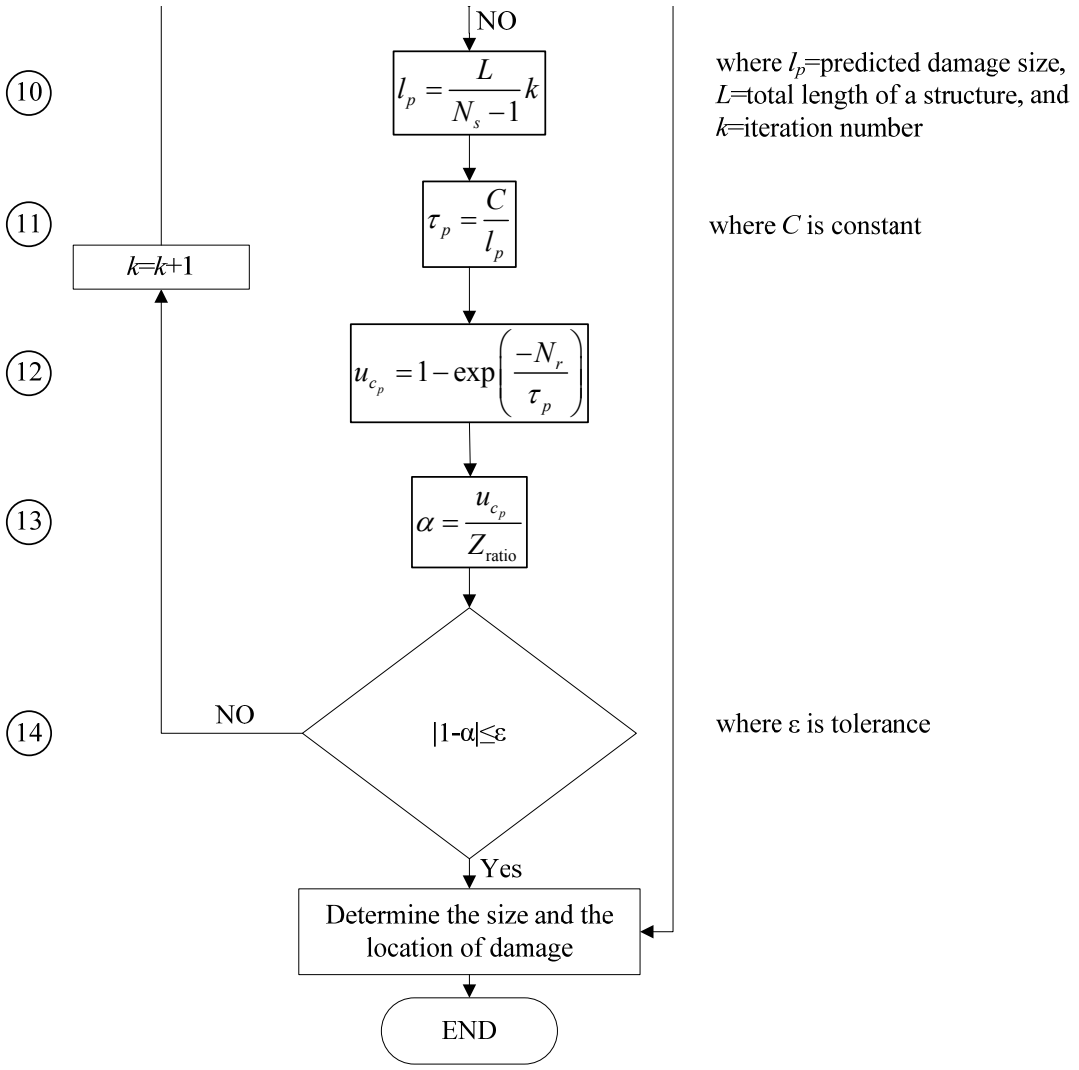

Fig. 5 Flow chart of the proposed Iterative Damage Index Method

For a structural element with a total length of L, the predicted damage size, ℓ_p, is given by

$$\ell_p = \frac{L}{N_s - 1}k \tag{16}$$

Next, the fitting function for the predicted damage size, u_{c_p}, is given by

$$u_{c_p} = 1 - \exp\left(\frac{-N_r}{\tau_p}\right) \quad \text{where } \tau_p = \frac{C}{\ell_p} \tag{17}$$

The ratio, α, is given by

$$\alpha = \frac{u_{c_p}}{Z_{\text{ratio}}} \tag{18}$$

If $|1-\alpha| \le \varepsilon$, where ε is the desired tolerance, the iterative processes stop. Based on a parametric study, we suggest to use $C = L_{eff}$, where L_{eff} is the effective length. For example, L_{eff} for a pinned-pinned boundary condition is equal to L, while L_{eff} for a fixed-free boundary condition is twice as long as L. Additional details can be found in You (2009).

2.3 Quantification of the accuracy of predicted damage

To quantify the accuracy of the predicted damage, two measures are introduced: e and Δ. The first measure is referring as the ratio between the actual damage size, s, and the predicted damage size, $\hat{s}$ divided by the s

$$\mathrm{e} = \frac{s - \hat{s}}{s} \tag{19}$$

The second measure is referring as the difference between the centers of the actual and the predicted damages divided by the total length of the structure, L

$$\Delta = \frac{c - \hat{c}}{L} \tag{20}$$

where c is the center of the actual damage, and $\hat{c}$ is the center of the predicted damage. The smaller the absolute values of both e and Δ are, the more accurate the damage detection is. If e and Δ are zero, then the damage is detected exactly. Note that e and Δ can be calculated for each damage detection model, where the damage detection model is specified N_r and N_s for the damage detection.

To generalize and compare the accuracy in the damage prediction for different damage cases, the damage detection percentage, γ, is calculated. For each damage detection model, γ is calculated as

$$\gamma = \frac{n_c}{n_t} \times 100 \ (\%) \tag{21}$$

where n_t is the number of total damage detection models and n_c is the number of correct damage predictions (i.e., e = 0 and Δ = 0) among the n_t cases. In addition, γ can be also calculated by applying various e and Δ to consider the error of predicted damage. Because various N_r cannot be used in experimental tests, the average of the e and Δ are calculated for the damage detection models with the only change of N_s. The average of the e and Δ will be used to compare how the damage detection methods perform in the experimental tests.

3. Validation using numerical data

This section refers two numerical examples to validate the proposed IDIM. FE model of a simply supported beam with hollow square section 0.05×0.05×0.01 m (2×2×½ in) and a FE model of a pedestrian bridge on the Texas A&M Golf Course at Texas A&M University, College Station, TX.

3.1 Simply supported beam

Table 1 summarizes the material and geometric properties for the simply supported beam. For the numerical simulation, the simply supported beam is constructed in ABAQUS (2004), including 280 beam elements with an equal width of 0.013 meters. From the modal analysis, the first three modeshapes are extracted and used in the DIM and IDIM. The first three eigenfrequencies are 11.205, 44.760, and 100.490 Hz.

Fourteen damage cases are studied to investigate the effect of various damage sizes, severities, and locations, as shown in Table 2. Note that the term of severity is defined as change in flexural rigidity. Cases 1, 2, and 3 are chosen to investigate the effect of damage size, while Cases 1, 4, 5, 6, and 7 are selected to investigate the effect of damage severity. Finally, Cases 8, 9, and 10 are selected to investigate the influence of different damage locations. The last four damage cases are selected to investigate the effect of multiple damage locations. Damage is simulated by reducing the modulus of elasticity of the appropriate elements.

The modeshapes can be obtained more accurately by increasing N_r which promises more reliable damage detection. However, it is necessary to decide on the minimum N_r for correct damage detection because one cannot use an unlimited N_r. Table 3 shows the minimum N_r to detect damage correctly (i.e., $\Delta = 0$ and $e = 0$) for all damage cases. It is apparent that a smaller N_r is needed for the IDIM than for the IDIM for most of damage cases. Therefore, the IDIM is generally more economical than the DIM in the simply supported beam.

The damage detection percentages for the simply supported beam are calculated by considering about ten thousand damage detection models (i.e., $n_t \approx 10{,}000$) with various N_r and N_s. N_r varies from five to 281 with the interval of four, while N_s changes from five to 449 with the interval of four. Table 4 summarizes those percentages for six of the fourteen damage cases. The results for the rest of the cases are similar. Five main observations can be made. First, the IDIM is typically more accurate than the DIM because the damage detection percentages of the IDIM are higher in most of the damage cases. Second, comparison of the Cases 1 and 2 shows that the IDIM is more efficient in estimating smaller damage associated with Case 1. Third, as shown in Cases 1 and 5, the more severe damage associated with Case 5 is estimated more accurately by the IDIM. Fourth, the similarity between Cases 1 and 9 implies that the damage location does not affect the relative accuracy of damage predictions. Finally, Cases 12 and 14 show that the IDIM is more accurate than the DIM in identifying the multiple locations of damage.

Cases 12 and 14 have two locations of damage, where the left location of damage is called ‘left damage’ and the right location of damage is referred as ‘right damage’ here. The Case 12 has different severities of damage while the severities of damage are same in the Case 14. Tables 5 to 6 show the values of γ for the two damage cases. From these tables, it is certain that the value of γ to detect the multiple damage is calculated by combining the value of γ to estimate the left damage with the value of γ to identify the right damage. Note that the value of γ to detect either the left damage or the right damage is higher than the value of γ to identify the multiple damage.

Table 1 Properties for a simply supported beam

Properties	Values
Length, L	3.56 m
Cross section area, A	974.19 mm²
Young's modulus, E	2.0×10^5 MPa
Poisson's ratio, ν	0.3
Second moment of cross-sectional inertia, I	3.11×10^5 mm^4
Density, ρ	7.85×10^3 kg/m³

Table 2 Damage scenarios of a simply supported beam

Damage Case	Damage size	Location		Severity[†]	Damage size	Location		Severity[a]
		From	To			From	To	
Undamaged	0.00 m	-	-	-	-	-	-	-
1	0.13 m	0.76 m	0.89 m	−20	-	-	-	-
2	0.25 m	0.76 m	1.02 m	−20	-	-	-	-
3	0.51 m	0.51 m	1.02 m	−20	-	-	-	-
4	0.13 m	0.76 m	0.89 m	−1	-	-	-	-
5	0.13 m	0.76 m	0.89 m	−10	-	-	-	-
6	0.13 m	0.76 m	0.89 m	−40	-	-	-	-
7	0.13 m	0.76 m	0.89 m	−60	-	-	-	-
8	0.13 m	0.00 m	0.13 m	−20	-	-	-	-
9	0.13 m	0.51 m	0.64 m	−20	-	-	-	-
10	0.13 m	1.65 m	1.78 m	−20	-	-	-	-
11	0.13 m	0.76 m	0.89 m	−20	0.13 m	2.54 m	2.67 m	−20
12	0.13 m	0.76 m	0.89 m	−20	0.13 m	2.54 m	2.67 m	−50
13	0.13 m	0.76 m	0.89 m	−50	0.13 m	2.54 m	2.67 m	−20
14	0.13 m	0.76 m	0.89 m	−50	0.13 m	2.54 m	2.67 m	−50

[a]Severity is defined as the change in flexural rigidity, expressed as Severity (%)=(EI^d−EI)/EI×100 where EI and EI^d are the flexural rigidities for the undamaged and damaged element, respectively

Table 3 The minimum number of recording points (N_r) and the minimum number of spline points (N_s) to detect damage accurately (Δ=0 and ϵ=0)

Damage Case	Minimum N_r (N_s)	
	DIM	IDIM
1	59 (113)	21 (29)
2	13 (29)	12 (15)
3	9 (15)	12 (15)
4	64 (85)	17 (29)
5	64 (113)	17(29)
6	40 (85)	10 (29)
7	40 (57)	14 (29)
8	22 (113)	74 (85)
9	N/A	12 (29)
10	58 (85)	5 (29)
11	78 (99)	29 (50)
12	N/A	50 99)
13	N/A	50 (99)
14	71 (99)	29 (50)

N/A: Damage cannot be detected

Table 4 Damage detection percentages with Δ=0 (unit is %)

Damage case		e										
		0	0.1	0.2	0.3	0.4	0.5	1.0	1.5	2.0	2.5	3.0
Case 1	DIM	0.81	15.3	51.6	69.1	77.5	80.4	86.5	92.0	94.4	94.6	96.4
	IDIM	5.35	67.5	79.4	82.9	84.6	86.7	95.5	95.6	95.7	96.4	99.6
Case 2	DIM	11.1	81.5	92.1	93.6	95.6	95.7	97.8	97.9	97.9	98.0	98.1
	IDIM	5.42	80.5	85.9	87.3	89.4	91.1	99.6	99.9	99.9	100	100
Case 5	DIM	0.17	12.1	48.2	65.3	74.3	77.7	83.7	89.4	91.7	92.0	93.8
	IDIM	1.47	25.7	72.4	83.3	85.3	87.9	95.5	95.6	95.8	96.3	99.6
Case 9	DIM	0.00	21.2	60.0	73.2	80.2	82.7	87.2	88.9	92.6	92.9	94.9
	IDIM	3.12	53.2	75.9	82.5	83.9	84.4	91.1	91.9	93.8	93.9	95.8
Case 12	DIM	0.00	0.00	0.00	1.38	12.3	22.3	67.0	67.0	67.0	67.0	67.0
	IDIM	8.39	61.4	71.2	75.9	78.5	81.6	89.6	90.2	93.7	95.7	95.8
Case 14	DIM	8.96	63.8	78.3	81.3	82.4	83.7	92.5	95.6	95.8	95.9	95.9
	IDIM	9.64	64.9	74.8	78.8	81.8	84.5	93.6	93.8	95.4	97.8	97.9

Table 5 Damage detection percentage Case 12 to detect (a) multiple damage, (b) left damage and (c) right damage (unit is %)

(a)

Δ		e										
		0	0.1	0.2	0.3	0.4	0.5	1.0	1.5	2.0	2.5	3.0
0	DIM	0.00	0.00	0.00	1.38	12.3	22.3	67.0	67.0	67.0	67.0	67.0
	IDIM	8.39	61.4	71.2	75.9	78.5	81.6	89.6	90.2	93.7	95.7	95.8

(b)

Δ		e										
		0	0.1	0.2	0.3	0.4	0.5	1.0	1.5	2.0	2.5	3.0
0	DIM	0.00	0.00	0.00	1.38	12.3	22.3	67.0	67.0	67.0	67.0	67.0
	IDIM	9.20	64.6	72.3	76.5	78.9	82.0	89.8	90.5	95.8	95.9	95.9

(c)

Δ		e										
		0	0.1	0.2	0.3	0.4	0.5	1.0	1.5	2.0	2.5	3.0
0	DIM	3.67	33.0	62.5	75.2	80.0	81.1	87.3	92.0	93.0	93.1	93.1
	IDIM	9.58	65.8	76.3	79.4	81.3	83.8	91.8	92.6	95.8	97.7	97.8

Table 6 Damage detection percentage Case 14 to detect (a) multiple damage, (b) left damage and (c) right damage (unit is %)

(a)

Δ		e										
		0	0.1	0.2	0.3	0.4	0.5	1.0	1.5	2.0	2.5	3.0
0	DIM	8.96	63.8	78.3	81.3	82.4	83.7	92.5	95.6	95.8	95.9	95.9
	IDIM	9.64	64.9	74.8	78.8	81.8	84.5	93.6	93.8	95.4	97.8	97.9

(b)

Δ		e										
		0	0.1	0.2	0.3	0.4	0.5	1.0	1.5	2.0	2.5	3.0
0	DIM	8.96	63.8	78.3	81.4	82.5	83.7	92.7	95.6	95.8	95.9	95.9
	IDIM	9.78	65.3	75.3	80.1	83.6	85.1	94.2	95.9	97.5	99.9	99.9

(c)

Δ		e										
		0	0.1	0.2	0.3	0.4	0.5	1.0	1.5	2.0	2.5	3.0
0	DIM	9.31	66.3	79.0	81.5	82.6	83.8	92.8	95.7	97.7	97.9	97.9
	IDIM	9.78	65.3	74.9	78.9	81.9	84.6	93.7	93.8	95.5	97.9	97.9

3.1 Pedestrian bridge

The pedestrian bridge, shown in Fig. 6, has a length of 9.04 meters, consists of two arched frames, a deck and bracings and other properties as summarized in Table 7. For the numerical validation, this pedestrian bridge is modeled in ABAQUS (2004) (see Fig. 7). A total of 2,674 beam elements are used to model the bridge with eight longitudinal beams. From the modal analysis, the first three bending modeshapes of the fourth longitudinal beam are extracted and used in the DIM and IDIM. The first three bending eigenfrequencies are 16.936, 24.310, and 33.499 Hz. We investigate ten damage cases analogous to those used for the previous numerical example. Table 8 summarizes those.

Table 7 Properties for a pedestrian bridge

Properties	Values
Length, L	9.04 m
Young's modulus, E	2.0×10^5 MPa
Poisson's ratio, ν	0.3
Density, ρ	10.13×10^3 kg/m³

Fig. 6 Pedestrian bridge in Texas A&M Golf Course at Texas A&M University, College Station, TX

Table 8 Damage scenarios for a pedestrian bridge

Damage Case	Damage size	Location		Severity[a]
		From	To	
Undamaged	0.000 m	-	-	-
1	0.078 m	2.47 m	2.55 m	−50
2	0.156 m	2.47 m	2.63 m	−50
3	0.311 m	2.47 m	2.78 m	−50
4	0.078 m	2.47 m	2.55 m	−10
5	0.078 m	2.47 m	2.55 m	−20
6	0.078 m	2.47 m	2.55 m	−70
7	0.078 m	2.55 m	2.63 m	−50
8	0.078 m	2.70 m	2.78 m	−50
9	0.078 m	3.02 m	3.09 m	−50
10	0.078 m	3.56 m	3.64 m	−50

[a]Severity is defined as the change in flexural rigidity, expressed as Severity (%)=(EI^d−EI)/EI×100 where EI and EI^d are the flexural rigidities for the undamaged and damaged element, respectively

Because the damage scenarios cannot be detected accurately (i.e., $\Delta = 0$ and $\varepsilon = 0$) by the two methods, $\Delta = 0.01$ and $\varepsilon = 0.1$ are used to determine the minimum N_r for all damage cases (see Table 9). Smaller N_r is required in the IDIM for all of the damage cases to achieve equivalent accuracy even with this less precise standard. Consequently, the IDIM also proves to be more economical than the DIM with the pedestrian bridge. The values of γ for the pedestrian bridge are calculated by considering about ten thousand damage detection models (i.e., $n_t \approx 10{,}000$) with various N_r and N_s. N_r varies from five to 449 with the interval of four, while N_s changes from five to 449 with the interval of four. Because the value of γ with $\Delta = 0$ are equal to zero, the error in estimating damage is considered (i.e., $\Delta = 0.01$). Table 10 summarizes those percentages for four damage cases among the ten cases, again because the results for the rest of the cases are not significantly different. The findings from those tables for the bridge are even more compelling than those for the beam. In particular, the damage detection percentages for the IDIM are higher across all damage cases.

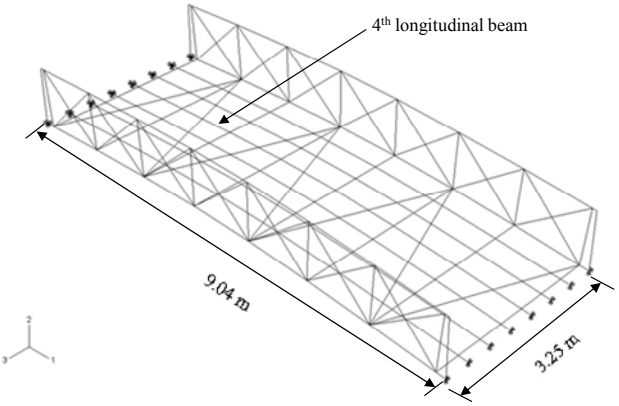

(a) top view

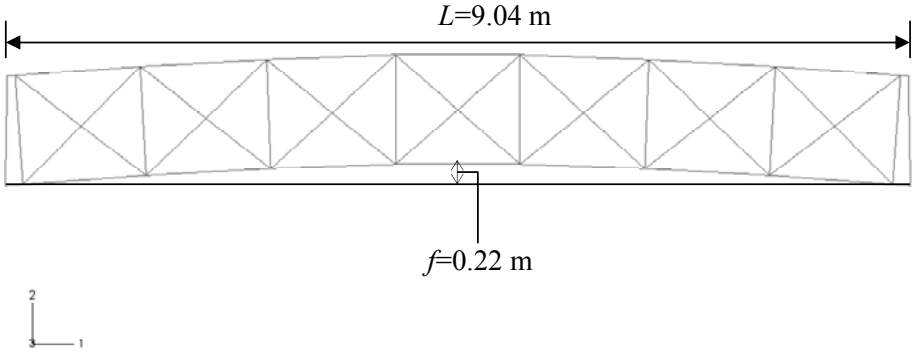

(b) side view

Fig. 7 Pedestrian bridge generated in ABAQUS (2004)

Table 10 Damage detection percentage with Δ=0.01 (unit is %)

Damage case		e										
		0	0.1	0.2	0.3	0.4	0.5	1.0	1.5	2.0	2.5	3.0
Case 1	DIM	0.00	0.00	0.00	0.00	0.00	0.00	3.39	26.3	52.2	62.2	67.3
	IDIM	0.00	4.50	7.88	13.0	17.3	21.9	37.5	49.1	59.6	68.7	76.1
Case 2	DIM	0.00	0.00	1.34	11.2	23.6	36.2	64.0	77.0	83.9	85.9	87.0
	IDIM	0.00	14.3	27.1	39.1	47.6	53.6	70.7	76.2	83.1	90.0	92.4
Case 5	DIM	0.00	0.00	0.00	0.00	0.00	0.00	2.08	19.2	49.2	61.7	67.2
	IDIM	0.00	3.97	7.21	11.5	15.5	18.9	36.2	49.7	56.6	63.8	72.3
Case 8	DIM	0.00	0.00	0.00	0.00	0.00	0.00	3.9	24.8	48.7	61.3	66.7
	IDIM	0.00	3.23	5.80	9.02	11.7	14.2	29.8	42.4	52.0	61.5	68.6

4. Validation using experimental data

The proposed method is also validated using experimental data with from real structures: a simply supported beam and a pedestrian bridge in the Texas A&M golf course, on the Texas A&M University campus in College Station, TX. The test data are obtained by a wireless monitoring system. Because a structure gradually deteriorates after its construction, the baseline of the beam and bridge (i.e., modeshapes for an undamaged structure) are obtained from the current structure.

4.1 Simply supported beam

The geometric and material properties of the beam are the same as those of the beam of considered in Section 3.1. The accelerations of the simply supported beam in the laboratory are measured from ten recording points from the left end of beam to the right one. The ten recording points are located with equal spacing (0.40 meters) on the beam. A steel plate with the weight of 0.6 kg (2.11% of the total mass of the beam) is placed between 0.787 meters and 0.889 meters from the left end of the beam to simulate a mass damage instead of a stiffness damage.

The experimental setup consists of a Wireless Sensor Network (WSN) (Reyer 2007) composed of a base station MIB510, MICA 2 motes and MTS310 sensor board. The beam is excited by an input hammer at 0.76 meters from the left end of the beam and the acceleration data are recorded with 250 Hz of sampling rate using the WSN. The first three modeshapes, shown in Fig. 8, are extracted from the measured accelerations by the Time Domain Decomposition (TDD) method, proposed by Kim *et al*. (2005).

For the limited number of MICA2 motes, three measuring sets (Set I, II, and III) and one reference point are used (see Fig. 9). The modes shapes obtained from the three sets are recalculated to match the reference point of each set. Note that the impact points in the three sets are identical. Fig. 10 shows a test set up for the Set I with five MICA 2 motes, the base station, and a lap-top computer.

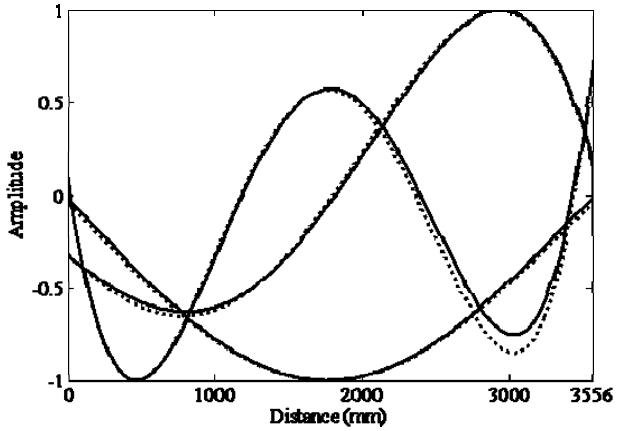

Fig. 8 The first three modeshapes for the simply supported beam (solid lines indicate the undamaged and dashed lines indicate the damaged)

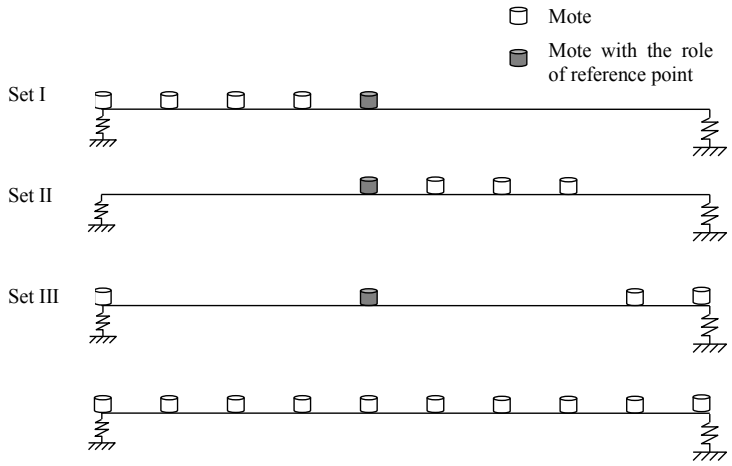

Fig. 9 Three measuring sets and a reference point for the simply supported beam

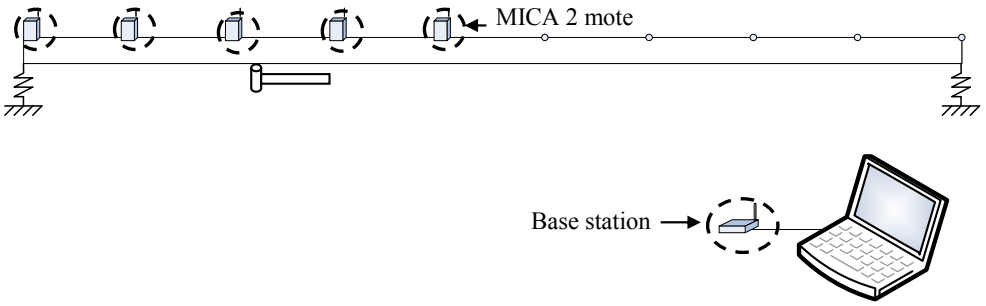

Fig. 10 Test set-up for the simply supported beam including MICA 2 motes, base station, and a lap-top computer

The average values of e and Δ are summarized in Table 11. From Table 11, we observe that the averages of Δ (the accuracy of pinpointing the location of damage) for the current DIM are practically the same as those of the proposed IDIM. However, the averages of the e for the proposed IDIM are around -3 while those of the current DIM are around -5. That means that the IDIM is 10% more accurate predicting the damage size than the DIM. Note that measurement noise was considered as acceleration data from actual measurements were used in this study.

Table 11 Average of e and Δ for a simply supported beam

		Range of N_s					
		10–100	101–200	201–300	301–400	401–500	501–1000
Average of Δ	DIM	0.037	0.037	0.037	0.037	0.037	0.037
	IDIM	0.042	0.045	0.045	0.045	0.045	0.045
Average of e	DIM	−4.88	−4.89	−4.89	−4.89	−4.89	−4.89
	IDIM	−2.99	−2.54	−2.48	−2.46	−2.45	−2.43

4.1 Pedestrian bridge

The geometric and material properties of the pedestrian bridge are the same as those of the pedestrian bridge considered in Section 3.2. The accelerations of the pedestrian bridge are measured at nine recording points. One point is located on the center of the 4th longitudinal beam of the bridge and eight other points are equally spaced (1.29 meters apart) on the 4th longitudinal beam of the bridge. To simulate a mass damage instead of a stiffness damage, three concrete blocks (81.66 kg or 2.46% of the total mass of the bridge) are added between 2.778 meters and 3.277 meters from one end of the bridge. The concrete blocks are located on the flat wood deck. The first three modeshapes, shown in Fig. 11, are obtained by the TDD. Because of the limited number of sensors, two measuring sets (Set A and B) and one reference point are also operated (see Fig. 12).

Table 12 summarizes the average of the e and Δ for the pedestrian bridge. From Table 12, it is found that the averages of Δ for the current DIM are practically the same as those of the proposed IDIM. However, the averages of e for the proposed IDIM are about −0.5 with only one being around −1, while those of the current DIM are all about −2. That means that the IDIM is 33% more accurate in estimating the damage size than the DIM.

Table 12 Average of e and Δ for a pedestrian bridge

		Range of N_s					
		10–100	101–200	201–300	301–400	401–500	501–1000
Average of Δ	DIM	−0.001	−0.002	−0.002	−0.002	−0.002	−0.002
	IDIM	0.012	0.015	0.015	0.015	0.015	0.015
Average of e	DIM	−2.27	−2.25	−2.25	−2.25	−2.25	−2.25
	IDIM	−0.92	−0.50	−0.47	−0.46	−0.45	−0.44

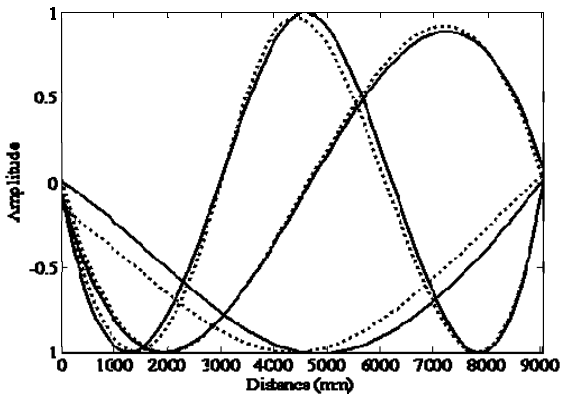

Fig. 11 The first three modeshapes for the pedestrian bridge (solid lines indicate the undamaged and dashed lines indicate the damaged)

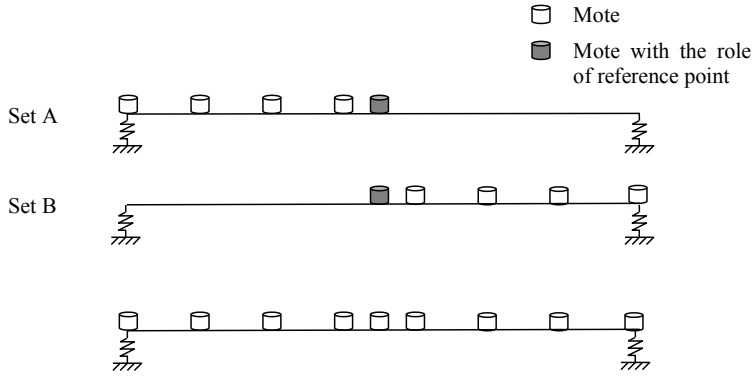

Fig. 12 Two measuring sets and one reference point for the pedestrain bridge

4. Conclusions

The proposed IDIM has both theoretical and practical advantages over the current DIM. It is a less arbitrary and more accurate vibration-based damage detection technique than the current DIM. Also, the proposed IDIM does not depend on a threshold, as required in the current DIM. Finally, the proposed IDIM is not affected by selected N_s.

Simulation and experimental comparisons demonstrate the superior performance of IDIM. Two parameters, e and Δ, are used to quantify the accuracy of predicted damage. Two example cases are studied to compare the DIM and the proposed IDIM: a simply supported beam and a pedestrian bridge at the Texas A&M golf course.

From simulation results with numerical models, five major findings emerge. First, the proposed IDIM is more economical than the DIM. Second, the proposed method is more accurate across various damage cases. Third, the proposed method is more efficient in identifying low magnitude

damage, which is rarely detected in practice. Fourth, the size of more severe damage is detected more correctly while the location of damage does not influence the accuracy of damage detection. Finally, the IDIM is more accurate than the DIM in estimating the multiple locations of damage.

The modeshapes are extracted from the two real structures by the TDD. Experimental tests with a simply supported beam and a pedestrian bridge show that the proposed IDIM is more accurate than the current DIM and that the proposed method can be applied successfully for structural health monitoring.

Acknowledgements

This work was supported partially by the Association of American Railroads (AAR). Opinions and findings presented are those of the authors and do not necessarily reflect the views of the sponsor.

References

ABAQUS (2004), *Version 6.5 User Manual*, Hibbit, Karlsson & Sorensen, Inc., Rhode Island, USA.

Alvandi, A. and Cremona, C. (2006), "Assessment of vibration-based damage identification techniques", *J. Sound Vib*., **292**(1-2), 179-202.

Bureau of Transportation Statistics (2008), *National transportation statistics*, U.S. Department of Transportation, Washington, DC, USA.

Choi, F., Li, J., Samali, B. and Crews, K. (2008), "Application of the modified damage index method to timber beams", *Eng. Struct.*, **30**(4), 1124-1145.

Huang, Q., Gardoni, P. and Hurlebaus, S. (2009), "Probabilistic capacity models and fragility estimates for reinforced concrete columns incorporating NDT data", *J. Eng. Mech. - ASCE*, **135**(12), 1384-1392.

Humar, J., Bagchi, A. and Xu, H. (2006), "Performance of vibration-based techniques for the identification of structural damage", *Struct. Health Monit*., **5**(3), 215-241.

Hurlebaus, S. and Gaul, L. (2006), "Smart structure dynamics", *Mech. Syst. Signal Pr.*, **20**(2), 255-281.

Kim, B., Stubbs, N. and Park, T. (2005), "A new method to extract modal parameters using output-only responses", *J. Sound Vib.*, **282**, 215-230.

Kim, C. and Kawatani, M. (2007), "Application of total squares algorithm for damage identification of bridges under a moving vehicle", *Proceedings of the 10th International Conference on Application of Statistics and Probability in Civil Engineering*, Tokyo, Japan, July.

Kim, J.T., Park, J.H. and Lee, B. (2007), "Vibration-based damage monitoring in model plate-girder bridges under uncertain temperature conditions", *Eng. Struct*., **29**(7), 1354-1365.

Kim, J.T., Ryu, Y., Cho, H. and Stubbs, N. (2003), "Damage identification in beam-type structures: frequency-based method vs mode-shape-based method", *Eng. Struct.*, **25**(1), 57-67.

Kim, J.T. and Stubbs, N. (2002), "Improved damage identification method based on modal information", *J. Sound Vib*., **252**(2), 223-238.

Kim, J.T. and Stubbs, N. (2003), "Nondestructive crack detection algorithm for full-scale bridges", *J. Struct. Eng. - ASCE,* **129**(10), 1358-1366.

Kim, J.T., Na, W., Ryu, Y., Park, J.H., Lee, J. and Lee, S. (2008), "Virbration-based damage monitoring algorithms for prestress-loss in PSC girder bridges", *Proceeding of SPIE*, **6932**, 69322C.

Kim, Y., Chong, J. and Kim, J. (2013), "Wavelet-based AR-SVM for health monitoring of smart structures", *Smart Mater. Struct*., **22**(1), 15003.

Lenzen, A. (2005), "Monitoring and damage assessment of mechanical systems by vibration analysis", *Proceedings of the 9th International Conference on Structural Safety and Reliability*, Rome, Italy, June.

Mizuno, Y., Monroig, E. and Fujino, Y. (2008), "Wavelet decomposition-based approach for fast damage detection of civil structures", *J. Infrastruct. Syst.*, **14**(1), 27-32.
Pandey, A.K., Biswas, M. and Samman, M.M. (1991), "Damage detection from changes in curvature mode shapes", *J. Sound Vib*., **145**(2), 321-332.
Pandey, A.K. and Biswas, M. (1994), "Damage detection in structures using changes in flexibility", *J. Sound Vib*., **169**(1), 3-17.
Park, J.H., Ho, D., Kim, J.T., Ryu, Y. and Yun, C. (2009), "Damage detection algorithm-embedded smart sensor node system for bridge structural health monitoring", *Proceeding of SPIE*, **7292**, 72922T.
Park, S., Stubbs, N., Bolton, R., Choi, S. and Sikorsky, C. (2001), "Field verification of the damage index method in a concrete box-girder bridge via visual inspection", *Comput. Aided Civil Infrastruct. Eng*., **16**, 58-70.
Reyer, M. (2007), *Design of a wireless sensor network for structural health monitoring of bridges*, Diplomarbeit**,** Institut für Angewandte und Experimentelle Mechanik, Universität Stuttgart, Stuttgart, Germany.
Shi, Z., Law, S. and Zhang, L. (2000), "Optimum sensor placement for structural damage detection", *J. Eng. Mech. - ASCE,* **126**(11), 1173-1179.
Stubbs, N. and Kim, J.H. (1996), "Damage localization in structures without baseline modal parameters", *Am. Inst. Aeronaut. J.*, **34**(8), 1644-1649.
Stubbs, N. and Park, S. (1996), "Optimal sensor placement for mode shapes via Shannon's sampling theorem", *Microcomput. Civil Eng.*, **11**(6), 411-419.
Wardhanam K. and Hadipriono, F.C. (2003), "Analysis of recent bridge failures in the United States", *J. Perform. Constr. Fac*., **17**(3), 144-150.
You, T. (2009), *Iterative damage index method for structural health monitoring*, Master thesis, Texas A&M University, College Station, Texas.
Zhang, Z. and Aktan, A.E. (1995), "The damage indices for constructed facilities", *Proceedings of the 13th International Modal Analysis Conference*, Nashville, Tennessee, February.